INS－T－510
[Accelerator－15]
August 1992

INSTITUTE FOR NUCLEAR STUDY
UNIVERSITY OF TOKYO
Tanashi, Tokyo 188
Japan

Analysis of Beam Feedback Loops of RF Acceleration System at TARN II

Takeshi Katayama

Institute for Nuclear Study, Univ. of Tokyo
3-2-1, Midori-cho, Tanashi Tokyo 188, Japan

Analysis of Beam Feedback Loops of RF Acceleration System at TARN II

Takeshi Katayama

Institute for Nuclear Study, Univ. of Tokyo
3-2-1, Midori-cho, Tanashi Tokyo 188, Japan

Abstract

Two beam-feedback-loops are prepared for the frequency control of RF acceleration system at cooler-synchrotron TARN II. One is the phase-loop and the other the radial-position-loop. In the present paper, the effects of these loops on the beam dynamics in the synchrotron are studied on the basis of Laplace transformation approach as well as the numerical values for the synchrotron acceleration at TARN II.

1. Introduction

At the RF acceleration of ion synchrotrons, the RF frequency should be varied largely since the injection energy of ions are normally low, several tens MeV/nucleon and the top energy is in the relativistic region. Hence the broadband electronic system is required for the low level RF system as well as for the high power amplifier and cavity. A commonly used master oscillator for this system, has been a type of Voltage Controlled Oscillator(VCO) where the output RF frequency is determined by the input voltage. Then the functional shape of input voltage to VCO, should be exactly corresponding to the change of revolution frequency of ions during the whole acceleration period. Otherwise the radial position of beam orbit is shifted from the central orbit and finally beams will be lost. For this purpose, at TARN II, a cooler synchrotron at INS, the pre-calculated input voltage to VCO, is stored in a memory module as a function of strength of bending magnetic field. It is read out at the unit increase of magnetic field strength and is applied to VCO through a digital to analogue converter. The deviation of thus obtained applied voltage from the ideal values,

should be as small as possible to accelerate the ion beams safely. Especially at the crossing of transition energy, the relative tolerance of the frequency error is around 10^{-5}. In spite of this tight requirement of RF frequency, however, there must inevitably exist FM noise, non-linearity and drift in the VCO, and the error of measuring the magnetic field strength. Moreover several noise sources will be included in the real circuit. They will bring out the RF frequency error and resultantly the synchronization between RF frequency and magnetic field will be broken.

Then any mechanism of correction of RF frequency should be devised for the stable synchrotron acceleration. The solution for this problem is to prepare the beam feedback loops, negative feedback loops to suppress the growth of distortion of orbit due to the error of RF frequency. Namely the shift of beam orbit due to the frequency error could be detected by the radial beam position monitor and its signal could be used for the correction of RF frequency. The first proposal of beam feedback loops was given in connection with the phase transition acceleration at CERN proton synchrotron[1,2], and the dynamic beam behaviour was investigated with an equivalent circuit analysis[3]. Thereafter, several RF systems were constructed mainly at the high energy proton synchrotrons[4,5,6], and recently the design method of RF control system was proposed with use of modern optimal control theory[7].

In the present paper, the analysis of beam behaviour under the feedback loops, are given in the framework of Laplace transformation approach. Firstly the outline of TARN II and its RF system are shortly described, and subsequently the mathematical formulae of the dynamics of bunch center are derived as well as the numerical values for TARN II ring.

TARN II is an experimental facility for accelerator studies and atomic-and nuclear-physics[8]. In addition to the functions of beam acceleration and slow extraction, it is equipped with electron cooling devices[9]. The main parameters of the ring are shown in Table 1. This cooler synchrotron has a maximum magnetic rigidity of 5.8 T-m, corresponding to a proton energy of 1.1 GeV. The ring is hexagonal, with an average diameter of 24.8 m. Its circumference is 77.76 m, or 17 times the extraction orbit of the injector cyclotron. It has 6 long, straight sections, each 4.2 m. They are used for the beam injection system, an RF cavity, an electron cooling device, and a slow beam-extraction system. It takes 3.5 s for the power supply to fully excite the whole magnet system. The flat-top duration of magnetic field is variable and is long enough for beam cooling and

extraction. The RF cavity can be tuned from 0.5 to 8.5 MHz and the power amplifier provides 5 kW, producing a gap voltage of 2 kV. The electron cooling system can cool an ion beam that has an energy of up to 200 MeV/u, corresponding to a maximum electron energy of 120 keV.

Table 1 Main Parameters of TARN II Ring

Maximum magnetic rigidity	5.8 T.m
Max. beam energy proton	1.1 GeV
ions with q/A = 1/2	370 MeV/u
Circumference	77.76 m
Average radius	12.376 m
Radius of curvature	4.045 m
Focusing structure	FBDBFO
Length of long straight section	4.20 m
Superperiodicity acceleration mode	6
cooling mode	3
Rising time of magnet excitation	3.5 s to full
Repetition rate (max)	0.1 Hz
Max. field of dipole magnets	15.0 kG
Max. gradient of quadrupole magnets	70 kG/m
Revolution frequency	0.31-3.75 MHz
Acceleration frequency	0.62-7.50 MHz
Harmonic number	2
Max. rf voltage	2 kV
Useful aperture	50×200 mm^2
Vacuum pressure	10^{-11} Torr

The lowest injection energy was chosen to be 2.58 MeV/u for $^{20}Ne^{4+}$ among the various ions from the sector-focused cyclotron, corresponding to the revolution frequency of 0.307 MHz in the TARN II ring. At the top energy of 1100 MeV for protons, the revolution frequency is 3.75 MHz; thus the ratio of the lowest to highest frequencies is around 11. The harmonic number was chosen to be 2, and the designed acceleration frequency is 0.6 MHz to 7.5 MHz. An acceleration voltage of 2 kV within the acceleration period of 3.5 s is sufficient

for a beam with an 0.5 % momentum spread. In Table 2, main RF parameters are listed.

Table 2 RF Accelerating Parameters

Injection energy	> 2.58 MeV/u
Acceleration energy	< 1.1 GeV
Momentum spread at injection	$< \pm 0.5\%$
Revolution frequency	0.31 ~ 3.75 MHz
Harmonic number	2
Acceleration frequency	0.62 ~ 7.50 MHz
Maximum RF accelerating voltage	2 kV

The RF cavity is a type of single-gap, ferrite-loaded, two-quarter-wave coaxial resonater. It covers the frequency range from 0.6 to 8.0 MHz by changing the ferrite bias current from 0 to 770 A. A power amplifier with a maximum output power of 5 kW can produce 2 kV of accelerating voltage throughout the whole frequency range[10].

The low-level RF electronics system (Fig. 1) is composed of a voltage-controlled oscillator (VCO) and several feedback loops. Three memory modules store the ramp data: RF frequency, acceleration voltage, and bias current as functions of bending-magnet field strength. At every 1-gauss increment, measured at the 25th dipole magnet for field monitoring, the data are read from memories and converted into analog voltage through digital-to-analog converters (DACs). The data are fed into a VCO, amplitude modulator, and bias current power supply, respectively. The error of bias current or equivalently the degree of cavity detuning, is detected as the phase difference between the RF signals at the grid and the plate of the final power tube. It is used for the correction of resonance frequency of cavity via a feedback loops (AFC). In addition, the signals of horizontal beam position (ΔR) and of the phase error ($\Delta\phi$) between beam bunch and acceleration RF field, are fed back to the voltage controlled oscillator for the correction of RF frequency. The output RF signal of this oscillator is fed to the driver-and power amplifiers.

During the beam injection period the VCO is phase-locked with the RF signal from a frequency synthesizer. The frequency and voltage in the injection period are finely adjusted for maximum capture efficiency. A track-and-hold circuit is inserted in this phase-locking loop to prevent the abrupt

variation of VCO frequency at the timing of change from synthesizer-locking to beam-locking.

In Fig. 2 the timing chart of RF system is illustrated. Triggering off the master pulse, the excitation of bending-and quadruple magnets, dB/dt-clock, feedback control gates, and other timing signals, are generated with the proper delays. Details of hardware of low level RF system are given elsewhere[11].

2. Principle of Beam Feedback Loops

In this chapter, the basic considerations on beam feedback loops are presented and the mathematical formulae, representing the beam behaviour with feedback loops, are derived.

2.1 Phase Lock Loop

At the synchrotron acceleration, first of all, the RF frequency should be exactly equal to the value of harmonic number times the revolution frequency of ions circulating just on the central orbit, during the whole acceleration period. Furthermore the phase difference between the center-of-bunch and the RF accelerating field, should be fixed during the acceleration period, otherwise the beam bunch would move along the RF field and would be lost due to the lack of phase stability. In other words, the RF field should be phase-locked to the beam bunch.

For these two purposes, the master oscillator is equipped with two beam feed-back loops, one is the ΔR feed back loop which corrects the error of RF frequency and the other the $\Delta\phi$ loop which works as the Phase Lock Loop (PLL). The essential parts of PLL[12] are a reference signal, a master oscillator, normally Voltage Controlled Oscillator (VCO), a loop filter and a phase detector (PD), of which the block diagram is illustrated in Fig. 3. Assuming that the phase detector is linear, the output voltage of PD is given by $V_D = K_D (\varphi_r - \varphi_0)$, where K_D $[volt/radian]$ is a constant of PD, and φ_r and φ_0 represent the phases of reference signal and the output signal of VCO, respectively. $F(s)$ is a transfer function of loop filter which determines the order of loop. The output frequency ω_0 of VCO is proportional to its control voltage V_0 and then $\omega_0 = K_V V_0$ where K_V is a constant of VCO with a dimension of [volt^{-1} · sec^{-1}]. Considering that the derivative of phase equals to the frequency, one obtains the relation of $\varphi_0(s) =$

ω_0/s with the Laplace transformation parameter s. Then the transfer function of VCO is

$$\frac{\varphi_0(s)}{V_0} = \frac{K_V}{s} . \qquad (2.1.1)$$

The closed loop transfer function from φ_r to φ_0 is given by

$$\frac{\varphi_0(s)}{\varphi_r(s)} = \frac{K_D K_V F(s)}{s + K_D K_V F(s)} . \qquad (2.1.2)$$

Suppose we choose the transfer function $F(s)$ as an integrator type, namely,

$$F(s) = K \frac{s + \omega_I}{s} , \qquad (2.1.3)$$

and then

$$\frac{\varphi_0(s)}{\varphi_r(s)} = 2\zeta\omega_n \frac{s + \omega_n / 2\zeta}{s^2 + 2\zeta\omega_n s + \omega_n^2} \qquad (2.1.4)$$

where $\zeta = \frac{I}{2}\sqrt{\frac{K K_D K_V}{\omega_I}}$ and $\omega_n = \sqrt{K K_D K_V \omega_I}$, respectively.

The numerical values of the absolute of $\varphi_0(s)/\varphi_r(s)$ are given in Fig. 4-a where the horizontal scale is the normalized angular frequency ω/ω_n. Curves in the figure correspond to various damping parameters ζ. When the reference phase $\varphi_r(t)$ is changed abruptly by the unit value as a step function, it's Laplace transformation is given by $\varphi_r(s) = 1/s$. In this case, the phase of VCO output $\varphi_0(t)$ is obtained using the inverse Laplace transformation of the equation (2.1.4). In Fig. 4-b, the changes of $\varphi_0(t)$ are illustrated against the normalized time $t_n = t/T_n$ where $T_n = 1/\omega_n$. Damping factor ζ is a parameter in the Figure. It is clearly seen that the phase of VCO signal tracks the phase of reference signal within the time interval of $\sim 4/\omega_n$ for the proper damping factor.

In the practical RF acceleration system, we should take into account the effects of beam transfer function with synchrotron oscillations and ΔR

feedback loop. In the following chapters, we will examine the characteristics of practical beam feedback loops on the basis of Laplace transformation method.

2.2 Synchrotron Oscillations

A particle subjected to an RF field in the ring, oscillates in the energy-and-phase domain, being called synchrotron oscillations. The equations of motion for this oscillations are given by

$$\frac{d}{dt}\left(\frac{\Delta E}{\Omega_0}\right) = \frac{\varepsilon e V}{2\pi}\left(\sin\phi - \sin\phi_S\right) \qquad (2.2.1)$$

and

$$\frac{d\phi}{dt} = h\,\Omega_0\,\xi\,\frac{\Delta E}{E_S}\,, \qquad (2.2.2)$$

where

$\Delta E = E - E_S$

E = total energy of ion (/ nucleon)

E_S = synchronous energy (/nucleon)

Ω_0 = revolution angular frequency of synchronous particle

ε = charge to mass ratio of ion (q / A)

V= peak voltage of RF field

ϕ = phase of ion relative to RF field

ϕ_S = synchronous phase

h = harmonic number

$\xi = \frac{1}{\beta_t^2}\left(\frac{1}{\gamma_t^2} - \frac{1}{\gamma_S^2}\right)$

γ_t = transition γ

β_S, γ_S = relativistic kinematical factor of synchronous particle

In the beam feedback theory, we do not treat each particle, but assume the bunch-of-beam as a rigid body, of which the center of gravity behaves as a single particle obeying the above synchrotron equations. It is a main subject of this feedback study whether the oscillations of the center of bunch are stable or not under the various acceleration conditions. In the present paper, we ignore

the effects of coherent oscillations due to, for example, the high current space charge force.

We should remark here about the definition of synchronous energy E_s and synchronous phase ϕ_s. Once the magnetic field B is given, the synchronous momentum p_s is given by

$$p_s = \varepsilon e B \rho_0 \tag{2.2.3}$$

where ρ_0 is the radius of curvature in the center of bending magnet. The synchronous energy E_s is deduced from the relation

$$E_s = \sqrt{(cp_s)^2 + (m_0 c^2)^2} \tag{2.2.4}$$

The angular frequency defined by

$$\omega_0 = h\beta_s c / R_0 \tag{2.2.5}$$

is an ideal RF frequency where R_0 is an average radius of central closed orbit in the ring. On the other hand, the synchronous phase ϕ_s is defined as

$$\sin \phi_s = 2\pi\rho_0 R_0 \dot{B} / V \tag{2.2.6}$$

where $\dot{B}$ is a time derivative of field strength in the bending magnets. If the RF voltage V and $\dot{B}$ change by ΔV and $\Delta\dot{B}$, respectively, the deviation of ϕ_s is given by

$$\Delta\phi_s = \tan \phi_s \left[\frac{\Delta\dot{B}}{\dot{B}} - \frac{\Delta V}{V} \right]. \tag{2.2.7}$$

Normally the change of $\dot{B}$ and V are considered to be small in the time range of period of synchrotron oscillations and $\Delta\phi_s$ can be neglected. Nevertheless, in the case that the high frequency component of ripple in the current of bending magnet is large, we should include these effects in the analysis.

The actual RF field produced in the cavity, differs from the ideal RF field in the frequency, phase and voltage. In Fig. 5 we show the relative relations of

real RF wave, ideal RF wave and the center of bunch, schematically. In the Figure, the phase difference between ideal and real RF's is denoted as u_0, and v means the phase of bunch-center on the real RF, and u_b the phase of bunch-center on the ideal RF. They are measured from the rising zero-crossing point. Then

$$u_b = u_0 + v \tag{2.2.8}$$

From the fact that the time derivative of phase is an angular frequency, one obtains

$$\frac{du_0}{dt} = \omega_{real} - \omega_{ideal}$$

$$\equiv - \Delta\omega_{rf} \tag{2.2.9}$$

With these new parameters, the phase equations for the center of bunch is given by

$$\frac{d}{dt}\left(\frac{\Delta E}{\Omega_0}\right) = \frac{\varepsilon eV}{2\pi}\left(\sin v - \sin \phi_s\right) \tag{2.2.10}$$

$$= \frac{\varepsilon eV}{2\pi}\left(v - \phi_s\right)\cos \phi_s \tag{2.2.11}$$

and

$$\frac{d}{dt}\left(u_0 + v\right) = - \frac{h\Omega_0^2}{\beta_s^2 E_s}|\eta|\,\Delta E$$

$$\equiv - K\,\Delta E/\Omega_0 \tag{2.2.12}$$

where the parameters K and η are defined as follows,

$$K \equiv \frac{h\Omega_0^2}{\beta_s^2 E_s}|\eta| \tag{2.2.13}$$

$$\eta = \left(1/\gamma_t^2 - 1/\gamma_s^2\right). \tag{2.2.14}$$

In the present text, we assume that the synchrotron is operated below the transition energy ($\gamma_s < \gamma_t$). To obtain the relation of (2.2.11) from (2.2.10), we use the linear approximation as

$$\sin \nu - \sin \phi_s = (\nu - \phi_s) \cos \phi_s \quad . \tag{2.2.15}$$

If we include the effect of change of ϕ_s by $\Delta\phi_s$, the equation is

$$\frac{d}{dt}\left(\frac{\Delta E}{\Omega_0} \right) = \frac{\varepsilon e V}{2\pi} (\nu - \phi_s - \Delta\phi_s) \cos \phi_s \quad . \tag{2.2.16}$$

Using the relation of $\dot{u}_0 \equiv - \Delta\omega_{rf}$, the phase equations become

$$\frac{d\nu}{dt} = - K \frac{\Delta E}{\Omega_0} + \Delta\omega_{rf}$$

and

$$\frac{d^2\nu}{dt^2} + \Omega_s^2 \nu = \Omega_s^2 \phi_s + \frac{d}{dt}\left(\Delta\omega_{rf} \right) \tag{2.2.17}$$

where Ω_s is a synchrotron-oscillation frequency defined by

$$\Omega_s^2 = \frac{h\Omega_0^2}{\beta_s^2 E_s} | \eta | \frac{\varepsilon e V}{2\pi} \cos \phi_s \quad . \tag{2.2.18}$$

For the phase parameter u_b, the equation is

$$\frac{d^2 u_b}{dt^2} + \Omega_s^2 u_b = \Omega_s^2 \left(\phi_s + u_0 \right) \tag{2.2.19}$$

where we use the relation of $u_b = u_0 + \nu$ and $\Delta\omega_{rf} = - \dot{u}_0$.
Furthermore by defining $\Delta\phi_\nu$ and $\Delta\phi_u$ as

$$\Delta\phi_\nu = \nu - \phi_s \tag{2.2.20}$$

$$\Delta\phi_u = u_b - \phi_s, \tag{2.2.21}$$

the phase equations of bunch center around the synchronous phase becomes

$$\frac{d^2\Delta\phi_v}{dt^2} + \Omega_s^2\Delta\phi_v = \frac{d}{dt}\left(\Delta\omega_{rf}\right) = -\ddot{u}_0 \tag{2.2.22}$$

$$\frac{d^2\Delta\phi_u}{dt^2} + \Omega_s^2\Delta\phi_u = \Omega_s^2 u_0 \tag{2.2.23}$$

which show that the phase oscillations of bunch center is a forced oscillations with external force of u_0. Here we assumed that the synchronous phase ϕ_s is constant during the time interval of present interest.

2.3 Beam Transfer Functions.

We introduce the Laplace transformation $f(s) = \int_0^\infty f(t)e^{-st}\,dt$ to convert the differential equations to algebraic equations. Also it gives the insight in the analysis in the frequency domain. The Laplace transformation of Eq. (2.2.22) is

$$(s^2 + \Omega_s^2)\Delta\phi_v(s) = s\Delta\omega_{rf}(s),$$

then

$$\Delta\phi_v(s) = \frac{s}{s^2 + \Omega_s^2}\Delta\omega_{rf}(s) \tag{2.3.1}$$

or

$$\Delta\phi_v(s) = -\frac{s^2}{s^2 + \Omega_s^2}u_0(s) \tag{2.3.2}$$

where we used the relation of

$$- u_0(s) \cdot s = \Delta\omega_{rf}(s)$$

Concerning with the variable of $\Delta\phi_u$, the Laplace transformation of Eq. (2.2.23) is

$$\Delta\phi_u(s) = -\frac{\Omega_s^2}{s^2 + \Omega_s^2} \cdot \frac{\Delta\omega_{rf}(s)}{s} \tag{2.3.3}$$

or

$$\Delta\phi_u(s) = \frac{\Omega_s^2}{s^2 + \Omega_s^2} u_0(s) \tag{2.3.4}$$

These two functions $\Delta\phi_v(s)$ and $\Delta\phi_u(s)$ are the beam transfer functions. Inserting $s = j\omega$ in the equation (2.3.2), we obtain the following form

$$\frac{\Delta\phi_v(\omega)}{u_0(\omega)} = \frac{\omega^2}{\omega_s^2 - \omega^2} \tag{2.3.5}$$

which shows that the amplitude of phase oscillations $\Delta\phi_v(\omega)$ will grows up rapidly to infinity if the frequency component of u_0 includes the synchrotron oscillation frequency Ω_s as is given in Fig. 6. The same argument can be applied for $\Delta\phi_u$ as is obvious from the equation (2.3.4).

The corresponding momentum spread, the Laplace transformed momentum spread $\Delta p/p(s)$, is derived with use of the relations (2.2.17) and the kinematical relation of

$$\frac{1}{\beta^2}\frac{\Delta E}{E} = \frac{\Delta p}{p} \tag{2.3.6}$$

as

$$\frac{\Delta p(s)}{p} = \frac{1}{h\Omega_s|\eta|} \frac{\Omega_s^2}{\Omega_s^2 + s^2} \Delta\omega_{rf}(s) \tag{2.3.7}$$

2.4 Requirement of Beam Feedback Loops

As is denoted in the preceding section, the phase difference $\Delta\phi_v(s)$ from the synchronous phase ϕ_s, is given by

$$\frac{\Delta\phi_v(s)}{u_0} = \frac{\omega^2}{\Omega_s^2 - \omega^2}$$

and the $\Delta\phi_v$ or corresponding momentum spread $\Delta p/p(s)$ grows up drastically if the forcing term $u_0(s)$ has the frequency component equal to synchrotron oscillations. At TARN II, the master source of the RF signal is VCO, and the allowable frequency shift is estimated with the formula of

$$\frac{\Delta\omega}{\omega_{ideal}} = \left(\frac{\gamma_t^2}{\gamma^2} - 1 \right) \frac{\Delta R}{R} \qquad (2.4.1)$$

The allowable change of average radius ΔR_{max} is assumed to be 5 mm, then

$$\left| \Delta\omega/\omega_{ideal} \right| \leq 9 \times 10^{-4}$$

where we used the numerical values of

$$R = 12.5\ m,\ \gamma_t \approx 1.8\ ,\ \gamma \approx 1$$

at the case of injection energy. When the beam feedback loops are not prepared, the actual RF frequency should track the ideal RF frequency within the accuracy of $\sim 1 \times 10^{-3}$. Considering the stability or linearity of VCO, the error of measuring magnetic field strength, the noise produced in the electric circuits etc, it is difficult to obtain the above accuracy. Furthermore when we accelerate the beam crossing the transition energy, it is obvious that the closed orbit shift becomes infinity at the transition energy even for the small frequency deviation. This is a reason why the beam feedback loops are prepared for the synchrotron acceleration.

3. Analysis of Feedback Loops

3.1 Internal Model

The Laplace transformation of Eqs. (2.2.11) and (2.2.12) gives the following two relations,

$$\frac{\Delta E}{\Omega_0} = \frac{1}{s}\frac{\varepsilon e V}{2\pi}\cos\phi_s \cdot \Delta\phi_v \tag{3.1.1}$$

and

$$\Delta\phi_v = \frac{1}{s}\left(- K\frac{\Delta E}{\Omega_0} + \Delta\omega_{rf} \right) \tag{3.1.2}$$

These relations give the internal model of interaction of beam and RF field and the block diagram of this model is given in Fig. 7.

The total feedback loops including the internal model, position feedback (ΔR), phase feedback ($\Delta\phi$), Voltage Controlled Oscillator (VCO) and programming signal from the function generator are schematically given in Fig. 8. The feedback voltage V_r through ΔR loop is given by

$$V_r = \Delta R \cdot N_r \cdot g_r \tag{3.1.3}$$

where $\Delta R[meter]$ is the output voltage from position monitor, $N_r[volt/meter]$ is a ΔR normalizer and g_r is a gain of controller including an integrator device. The feedback voltage V_p through $\Delta\phi$ loop is given by

$$V_p = \Delta\phi_v \cdot G_d \cdot g_p \tag{3.1.4}$$

where $\Delta\phi_v$ is a phase difference $(v - \phi_s)$ from the synchronous phase, $G_d[volt/radian]$ is a sensitivity of phase detector and g_p is a gain of phase loop controller. V_{pr} represents the programmed voltage which gives the ideal RF frequency from VCO, and ΔV_{pr} is the difference of real programmed voltage from the ideal programmed voltage. The total voltage applied to VCO is then

$$Vvco = V_{pr} + \Delta V_{pr} - V_r - V_p \tag{3.1.5}$$

and the output frequency from VCO is

$$\omega_{rf} = G_0 Vvco \tag{3.1.6}$$

where $G_0[rad/volt]$ is a constant of VCO. Considering that the ideal RF frequency is given by $\omega_{ideal} = G_0 \cdot V_{pr}$ and the noise component $\Delta\omega_d$ is mixed, the $\Delta\omega_{rf}$ applied to the input of internal model is then,

$$\Delta\omega_{rf} = G_0 \left(- \Delta\phi_v \cdot G_d \cdot g_p - \Delta R \cdot N_r \cdot g_r + \Delta V_{pr} \right) + \Delta\omega_d \qquad (3.1.7)$$

In the real circuit, the low pass filters are inserted in the ΔR and $\Delta\phi$ loops, however, in the present analysis, we ignore the effects of these low pass filters.

3.2 Open Loop Characteristics

When two feedback loops are open, the following equations represent the behavior of the system.

$$\left(\Delta\omega_{rf} - K \frac{\Delta E}{\Omega_0} \right) \frac{1}{s} = \Delta\phi_v \qquad (3.2.1)$$

$$\Delta\phi_v \cdot \frac{\varepsilon e V}{2\pi} \cos\phi_s \cdot \frac{1}{s} = \frac{\Delta E}{\Omega_0} \qquad (3.2.2)$$

$$\frac{\Delta E}{\Omega_0} \cdot \frac{\Omega_0}{\beta^2 E} \hat{\eta} = \Delta R \qquad (3.2.3)$$

where the last equation gives the closed orbit shift ΔR at the beam position monitor of local dispersion $\hat{\eta}$. From these relations, two important relations

$$\frac{\Delta\phi_v(s)}{\Delta\omega_{rf}} = \frac{s}{s^2 + \Omega_s^2} \qquad (3.2.4)$$

and

$$\frac{\Delta R(s)}{\Delta\omega_{rf}} = \frac{1}{h\Omega_0} \frac{\hat{\eta}}{|\eta|} \frac{\Omega_s^2}{\Omega_s^2 + s^2} \qquad (3.2.5)$$

are obtained. Again one can easily understand that the phase shift and the corresponding closed orbit shift become infinity at $\omega = \Omega_s$.

By applying the inverse Laplace transformation to the above obtained $\Delta R(s)$ and $\Delta\phi(s)$ relations, we obtain the relations in the time domain. The indicial response of the system, namely behavior of the system due to the step variation of $\Delta\omega_{rf}$, is derived with the Laplace transformation of $\Delta\omega_{rf}$ as

$$\Delta\omega_{rf} \cdot \frac{1}{s}, \tag{3.2.6}$$

and then

$$\frac{\Delta R(s)}{\Delta\omega_{rf}} = \frac{1}{h\Omega_0} \frac{\hat{\eta}}{|\eta|} \frac{\Omega_s^2}{s^2 + \Omega_s^2} \frac{1}{s}. \tag{3.2.7}$$

The inverse transformation gives the form of non-damping oscillations as

$$\frac{\Delta R(t)}{\Delta\omega_{rf}} = \frac{\hat{\eta}}{h\Omega_0|\eta|}\left(1 - \cos(\Omega_s t)\right), \tag{3.2.8}$$

which shows the maximum deviation of $\Delta R(t)$ is

$$\Delta R_{max} = \frac{2\Delta\omega_{rf}\hat{\eta}}{h\Omega_0|\eta|} \tag{3.2.9}$$

The numerical values of $\Delta R_{max}/\Delta f_{rf}$ at the open loop conditions are calculated against various beam energy in Figs. 9 and 10, where the parameters concerning RF acceleration are plotted against the acceleration time. In both figures, the strength of magnetic field at the injection and the top periods are 0.2 Tesla and 1.5 Tesla, respectively. In the case of ion beams of charge-to-mass ratio q/A = 0.5 (Fig. 9), the injection energy is 10 MeV/u and the top energy is 370 MeV/u. The frequency of synchrotron oscillations changes from roughly 1 kHz to 400 Hz. The maximum shift of closed orbit ΔR due to the step error of RF frequency by Δf_{rf}, has the maximum value 23 mm/kHz at the injection energy and decreases gradually. On the other hand, in the case of proton acceleration, the injection energy is 40 MeV and the top energy is 1100 MeV. It should cross the transition energy at 800 MeV where the synchrotron oscillation frequency

becomes zero and the shift of closed orbit due to the error of RF frequency reaches infinity without the feedback loops.

3.3 Closed Loops Characteristics

3.3.1 Phase Loop

When the phase loop is closed, the error of RF frequency $\Delta\omega_{rf}$ is given by

$$\Delta\omega_{rf} = G_0\left(- \Delta\phi_v \cdot G_d \cdot g_p + \Delta V_{pr} \right) + \Delta\omega_d \qquad (3.3.1)$$

Using the following relation of internal model,

$$\frac{\Delta\phi_v(s)}{\Delta\omega_{rf}} = \frac{s}{s^2 + \Omega_s^2},$$

one obtains the transfer function of closed $\Delta\phi_v$ loop as

$$\Delta\phi_v(s) = \frac{s}{s^2 + G_0 G_d g_p s + \Omega_s^2}\left(G_0\Delta V_{pr} + \Delta\omega_d\right) \qquad (3.3.2)$$

or

$$\Delta\phi_v(s) = \frac{s}{s^2 + 2\zeta\Omega_s s + \Omega_s^2}\left(G_0\Delta V_{pr} + \Delta\omega_d\right) \qquad (3.3.3)$$

where we define the damping factor ζ as

$$2\zeta\Omega_s \equiv G_0 G_d g_p . \qquad (3.3.4)$$

Indicial response of this system for various damping factor ζ are obtained and the time domain behavior of the system is given as follows;

Case I : $|\zeta| > 1$

The roots of characteristics equation, $s^2 + 2\zeta\Omega_s s + \Omega_s^2 = 0$, are two real values

$$\alpha = \left(-\zeta + \sqrt{\zeta^2 - 1} \right) \Omega_s$$

$$\beta = \left(-\zeta - \sqrt{\zeta^2 - 1} \right) \Omega_s .$$

Then the indicial response of the system is given in the time domain as,

$$y_1(t) = 1 + \frac{1}{2\sqrt{\zeta^2 - 1}} \left\{ \left(-\zeta - \sqrt{\zeta^2 - 1} \right) e^{\sqrt{\zeta^2 - 1}\,\Omega_s t} - \left(-\zeta + \sqrt{\zeta^2 - 1} \right) e^{-\sqrt{\zeta^2 - 1}\,\Omega_s t} \right\}$$

$$\times e^{-\zeta \Omega_s t} \qquad (3.3.5)$$

Case II : $|\zeta| = 1$

In this case, the system is in the critical damping condition and the solution is

$$y_2(t) = 1 - e^{\mp \Omega_s t} \left(1 \mp \Omega_s t \right) \qquad (3.3.6)$$

where $\mp$ signs correspond to the case of $\zeta = \pm 1$.

Case III : $0 \le |\zeta| < 1$

The indicial response is represented in the time domain as

$$y_3(t) = 1 - \frac{1}{\sqrt{1 - \zeta^2}} e^{-\zeta \Omega_s t} \sin \left\{ \left(\sqrt{1 - \zeta^2}\, \Omega_s t \right) + \varphi \right\} \qquad (3.3.7)$$

$$\varphi = \tan^{-1} \left(\sqrt{1 - \zeta^2} / \zeta \right)$$

From these solutions, one can easily understand that the system will diverge for the negative value of ζ.

The phase loop regulates the beam phase $\Delta\phi$ and resultantly, it also controls the beam position via a relation of

$$\frac{\Delta R(s)}{\Delta \phi_v(s)} = \frac{1}{s} \frac{\Omega_s^2}{h \Omega_0} \frac{\hat{\eta}}{|\eta|} \qquad (3.3.8)$$

which is obtained from the relations (3.2.4) and (3.2.5).
For example, the indicial response of ΔR in the time domain, is given by

$$\frac{\Delta R(t)}{\Delta \omega_{rf}} = \frac{\hat{\eta}}{h\Omega_0 |\eta|}\left[1 - \frac{1}{\sqrt{1-\zeta^2}} e^{-\zeta\Omega_s t} \sin\left\{ \left(\sqrt{1-\zeta^2}\,\Omega_s t \right) + \varphi \right\} \right]$$

$$\tan\varphi = \frac{\sqrt{1-\zeta^2}}{\zeta}$$

in the case of $1 \geq |\zeta| > 0$.

Numerical values at the injection energy are given in Fig. 11 for various ζ values. As is obvious, the system is open loop for $\zeta = 0$ and it corresponds to the results of preceding section. Again the beam position diverge for negative value of ζ and converge for $\zeta > 0$. However we should notice that the values of $\Delta R(t \to \infty)$ becomes

$$\frac{\Delta R(\infty)}{\Delta \omega_{rf}} = \frac{\hat{\eta}}{h\Omega_0 |\eta|} \qquad (3.3.9)$$

even in the case of convergence. It means that it has the offset value.

The characteristics of phase loop in the frequency domain is obtained by putting $s = j\omega$ in the relation (3.3.3) as

$$\left| \frac{\Delta\phi_V(\omega)}{\Delta \omega_{rf}} \right| = \frac{\omega}{\sqrt{\left(\Omega_s^2 - \omega^2 \right)^2 + 4\zeta^2\Omega_s^2\omega^2}} \qquad (3.3.10)$$

and the resultant ΔR characteristics via phase loop is

$$\left| \frac{\Delta R(\omega)}{\Delta \omega_{rf}} \right| = \frac{\hat{\eta}}{h\Omega_0 |\eta|} \frac{\Omega_s^2}{\sqrt{\left(\Omega_s^2 - \omega_s \right)^2 + 4\zeta^2\Omega_s^2\omega^2}} \qquad (3.3.11)$$

This relation is numerically given in Fig. 12, where we can see that in the low frequency region the radial shift is almost constant as

$$\left|\frac{\Delta R(\omega)}{\Delta \omega_{rf}}\right| \sim \frac{\hat{\eta}}{h\Omega_0|\zeta|} \qquad (3.3.12)$$

whereas in the frequency region larger than $\omega > \Omega_s$, the shift decreases rapidly. In other words, the phase loop is effective for the large frequency region, and does not work at the low frequency region.

3.3.2 Radial loop

With use of radial loop only, the RF frequency error $\Delta\omega_{rf}$ is given as

$$\Delta\omega_{rf} = - G_0 \Delta R \cdot N_r \cdot g_r + G_0 \Delta V_{pr} + \Delta\omega_d \qquad (3.3.13)$$

and the beam transfer function $\Delta R(s)$ is given by

$$\Delta R(s) = \frac{\hat{\eta}}{h\Omega_0|\eta|} \frac{\Omega_s^2}{s^2 + \Omega_s^2 + AG_0N_r g_r(s)} \qquad (3.3.14)$$

where $A = \dfrac{\Omega_s^2 \hat{\eta}}{h\Omega_0|\eta|}$ and $g_r(s)$ is the transfer function of radial loop gain. As is clear from the characteristic equation

$$s^2 + \Omega_s^2 + AG_0N_r g_r(s) = 0 , \qquad (3.3.15)$$

if $g_r(s)$ is independent of s, the characteristic equation has two roots of real values, one is the positive and the other the negative. Then $\Delta R(s)$ does not have damping terms.

There are several choices of the type of $g_r(s)$, one is the proportional-and-integration type

$$g_r(s) = K_r \frac{1 + T_r s}{T_r s} \qquad (3.3.16)$$

and the other is of low pass filter type,

$$g_r(s) = K_r \frac{1}{1 + T_r s} \tag{3.3.17}$$

For the proportional-and-integration type, the characteristics equation has the form of trigonometric equation,

$$s^3 + \Omega_s^2 (1 + \kappa) s + \frac{1}{T_r} \Omega_s^2 \kappa = 0 \tag{3.3.18}$$

where

$$\kappa \equiv G_0 N_r K_r \frac{1}{h \Omega_0} \frac{\hat{\eta}}{|\eta|}. \tag{3.3.19}$$

This equation has at least one positive real solution and hence the system will be unstable. This situation is explained also by the Routh-Hurwitz method, which gives the condition for stable system as follows. If the characteristic equation is of the form,

$$a_0 s^3 + a_1 s^2 + a_2 s + a_3 = 0 \tag{3.3.20}$$

the stable condition is

$$a_0, a_1, a_2, a_3 > 0 \tag{3.3.21}$$

and the matrix

$$\begin{vmatrix} a_1 & a_0 \\ a_3 & a_2 \end{vmatrix} > 0 \tag{3.3.22}$$

In the present situation, it is easily found that both conditions are contradicted and the system is unstable.

If one selects the low pass filter type, then the characteristic equation has the form of

$$s^3 + \frac{1}{T_r} s^2 + \Omega_s^2 s + \frac{1}{T_r} \Omega_s^2 (1 + \kappa) = 0 \qquad (3.3.23)$$

The Routh-Hurwitz condition is given by

$$0 > \kappa > -1 \qquad (3.3.24)$$

This condition is satisfied by the proper choice of gain of radial loop, however the range of stable region is found to be quite small and is not adequate for the stable operation of the synchrotron acceleration.

3.3.3 Phase and Radial loops

As is explained in the preceding section, the phase loop alone is inadequate for the low frequency region, and the radial loop can not satisfy the broad stable region. Then the combination of phase and radial loops is used for the TARN II operation. Following the same process in the preceding section, one obtains

$$\Delta\omega_{rf} = G_0 \left(- \Delta\phi \cdot G_d \cdot g_p - \Delta R \cdot N_r \cdot g_r + \Delta V_{pr} \right) + \Delta\omega_d \qquad (3.3.25)$$

and, with use of the relations of internal model

$$\frac{\Delta R}{\Delta \phi_v} = \frac{A}{s}$$

$$\frac{\Delta R}{\Delta \omega_{rf}} = \frac{A}{s^2 + \Omega_s^2}$$

one obtains the transfer function

$$\Delta R(s) = \frac{\left(G_0 \, \Delta V_{pr} + \Delta\omega_d \right) A}{s^2 + G_0 \, G_d \, g_p \, s + \Omega_s^2 + G_0 \, A \, N_r \, g_r} \qquad (3.3.26)$$

and

$$\Delta\phi_v(s) = \frac{s\left(G_0\,\Delta V_{pr} + \Delta\omega_d\right)}{s^2 + G_0\,G_d\,g_p\,s + \Omega_s^2 + G_0\,A\,N_r\,g_r} \tag{3.3.27}$$

, respectively.

At TARN II, the phase gain control g_p is constant as

$$g_p(s) \equiv K_p$$

and the radial gain control is

$$g_r(s) \equiv K_r \frac{1 + T_r\,s}{T_r\,s} .$$

We choose the integrator time constant $T_r = \frac{1}{\Omega_{s0}}$ where Ω_{s0} is the synchrotron angular frequency at the injection energy. The transfer functions are written as

$$\frac{\Delta R(s)}{\Delta\omega_{rf}} = \frac{s\,\Omega_s^2}{s^3 + 2\zeta\Omega_{s0}s^2 + (1+\kappa)\Omega_s^2 s + \Omega_s^2\Omega_{s0}\kappa} \cdot \frac{\widehat{\eta}}{h\Omega_0|\eta|} \tag{3.3.28}$$

and

$$\frac{\Delta\phi_v(s)}{\Delta\omega_{rf}} = \frac{s^2}{s^3 + 2\zeta\Omega_{s0}s^2 + (1+\kappa)\Omega_s^2 s + \Omega_s^2\Omega_{s0}\kappa} \tag{3.3.29}$$

where $$G_0 G_d K_p \equiv 2\zeta\Omega_{s0} . \tag{3.3.30}$$

The characteristic equation is

$$s^3 + 2\zeta\Omega_{s0}\,s^2 + (1+k)\,\Omega_s^2\,s + \Omega_s^2\,\Omega_{s0}\,\kappa = 0 \tag{3.3.31}$$

From the Routh-Hurwitz condition, the parameter ζ and κ should obey the following condition for the stable system,

$$\zeta > 0 , \ \kappa > 0 \tag{3.3.32}$$

and

$$\zeta > \frac{\kappa}{2(1+\kappa)} \qquad (3.3.33)$$

If one choose $\zeta > 0.5$, the system is stable for the any value of κ under the condition that it is positive. Now the indicial response of $\Delta R(s)$ is given by

$$\frac{\Delta R(s)}{\Delta \omega_{rf}} = \frac{\Omega_s^2}{s^3 + 2\zeta\Omega_{s0}\, s^2 + (1+\kappa)\Omega_s^2\, s + \Omega_s^2\, \Omega_{s0}\, \kappa} \frac{\hat{\eta}}{h\,\Omega_0 |\eta|} \qquad (3.3.34)$$

and the inverse Laplace transformation gives the behaviour in the time domain. Assuming the three solutions of the characteristic equation as α, β and γ, then the solution of time domain is

$$\frac{\Delta R(t)}{\Delta \omega_{rf}} = \frac{\hat{\eta}}{h\Omega_0 |\eta|}\, \Omega_s^2 \times$$

$$\left[\frac{1}{(\beta-\alpha)(\gamma-\alpha)} e^{\alpha t} + \frac{1}{(\gamma-\beta)(\alpha-\beta)} e^{\beta t} + \frac{1}{(\alpha-\gamma)(\beta-\gamma)} e^{\gamma t} \right] \qquad (3.3.35)$$

One can easily understand that if one of α, β, γ has the positive real part, the system is unstable.

The offset value of ΔR for the indicial response is evaluated by means of the final value theorem of Laplace transformation, which states

$$\lim_{t\to\infty} \Delta R(t) = \lim_{s\to 0} s\, \Delta R(s)$$

$$= 0 \quad (\kappa > 0) \qquad (3.3.36)$$

This advantage, no offset, is one of the reason why we select the radial loop gain g_r as proportional-integration type.

Near the transition energy, $|\eta|$ becomes zero and the shift of the closed orbit reaches infinity, and the acceleration is impossible without the beam feedback loops. However, if one uses the phase and radial feedback loops, the indicial response of $\Delta R(s)/\Delta\omega_{rf}$ becomes at the limit $\gamma \to \gamma_t$, to the following value

$$\lim_{\gamma \to \gamma_t} \frac{\Delta R(s)}{\Delta \omega_{rf}} = \frac{1}{s + \Omega_{s0}} \frac{1}{G_0 N_r K_r} \tag{3.3.37}$$

and the inverse Laplace transformation gives the time domain solution at $\gamma = \gamma_t$ as

$$\frac{\Delta R(t)}{\Delta \omega_{rf}} = \frac{1}{G_0 N_r K_r} e^{-\Omega_{s0} t} \tag{3.3.38}$$

which means that even at the transition energy, the closed orbit shift is within the finite value of $\sim \frac{1}{G_0 N_r K_r}$.

In Figs. 9 and 10, the numerical values of closed orbit shift $\Delta R / \Delta f_{rf}$ are given as a function of acceleration time. Typical loop parameters of $\zeta = 0.6$ and $K_r = 5 \times 10^{-3}$, 5×10^{-2} are selected in these fingers. The closed orbit shift $\Delta R / \Delta f_{rf}$ could remain within 1 mm/kHz with the strong radial loop gain. Even at the transition energy, the closed orbit shift remains small value, contrasting with the results at the open loop in the same figure.

3.3.4 Frequency Analysis of Transfer Function

From the relation (3.3.28) one obtains the frequency response of the transfer function by putting $s = j\omega$ as

$$y(\omega) = \frac{j \omega \Omega_s^2}{-2\zeta \Omega_{s0} \omega^2 + \Omega_s^2 \Omega_{s0} \kappa - j\left(\omega^3 - \Omega_s^2 (1 + \kappa) \omega\right)} \tag{3.3.39}$$

where $y = \frac{\Delta R}{\Delta \omega_{rf}} / \frac{\hat{\eta}}{h \Omega_0 |\eta|}$

and the absolute value of $y(\omega)$ is derived as

$$|y(\omega)| = \frac{x}{\sqrt{\left(\kappa - 2\zeta x^2\right)^2 \delta^2 + \left(x^2 - (1 + \kappa)\right)^2 x^2}} \tag{3.3.40}$$

where $x = \omega / \Omega_s$ and $\delta = \Omega_{s0} / \Omega_s$.

In Fig. 12, the numerical values of $|y(\omega)|$ for typical parameters $\zeta = 0.6$ and $K_r = 5 \times 10^{-3}$ are given for the injection energy 10 MeV/u and the top energy 370 MeV/u as well as the values at no radial feedback, $K_r = 0$. One can clearly find that the radial shifts of closed orbit due to the RF frequency error, are effectively suppressed by the proper selection of the values of ζ and K_r respectively.

4. Conclusive Remarks

In the present paper, dynamics of bunch center during the RF acceleration are investigated theoretically with Laplace transformation approach and numerical values are given in the case of cooler synchrotron TARN II. The coherent motion of bunches due to the space charge effects, are ignored in the present analysis. It is found that the combined use of two beam feedback loops, a radial position feedback and a phase feedback loop, will suppress the shift of closed orbit due to the error of RF frequency, dR/df_{RF}, within several mm/kHz with the proper selection of feedback strength. The damping parameter ς in the phase loop should be positive value and is selected at 0.6 ~ 1.0. The strength of radial feedback loop K_r can be chosen as large value as possible for the stable dynamic system. However in the real circuit, too large K_r will introduce the parastic- or self excited oscillations in the loop and would not be adequate for the beam acceleration. Then as a typical example, K_r is selected between 0.005 to 0.05 in the present analysis. With these parameters, the beam will be steadily accelerated even at the crossing of transition energy.

The white noise included in the voltage to VCO, the low pass filter and the delay of signals due to the finite length of cables and circuits, would modify the results obtained in the present analysis. However these effects will be second order in the real RF system and be the subjects to be investigated hereafter.

5. Acknowledgement

The author would like to express his sincere thanks to Prof. S. Ninomiya for the discussion on various aspects of feedback theory. Dr. S. Watanabe, Mr. T. Watanabe, Mr. M. Yoshizawa and Dr. M. Kanazawa are acknowledged for their collaboration on the construction and operation of RF system.

6. References

[1] K. Johnsen and C. Schmeltzer, "Beam Controlled Acceleration in Synchrotrons", Proc. of CERN Symposium (1956) p. 395

[2] W. Schnell, "Remarks on the Phase Lock System of the CERN Proton Synchrotron", Proc. of CERN Acc. Conference (1959) p. 485

[3] W. Schnell, "Equivalent Circuit Analysis of Phase Lock Beam Control System", (1968) CERN 68-27

[4] U. Bigliani et al., "The RF Accelerating System for the CERN PS Booster", IEEE Trans. NS-18, No. 3 (1971) p. 233

[5] M. Kondoh et al., "RF Acceleration in KEK Booster", IEEE Trans. NS-24, No. 3 (1977) p. 1533

[6] K. G. Meisner et al., "A New Low Level RF System for the Fermilab Booster", IEEE Trans. NS-26, No. 3 (1979) p. 4061

[7] T. Yamagishi, "Study on the Design Method of RF Acceleration System of Ion Synchrotron" (1992) thesis, Univ. of Tokyo

[8] T. Katayama et al., " Cooler Synchrotron TARN II", Particle Accelerators, Vol. 32 (1990) p. 105

[9] T. Tanabe et al., " Electron Cooling Experiments at INS" , Nucl. Instrum. Meth. A307 (1991) p.7

[10] K. Satho et al., " Broadband Accelerating Cavity for TARN II", Proc. of the 6th Symp. on Acc. Science and Technology, Tokyo(1987) p. 117

[11] T. Katayama et al., "RF Accelerating System for TARN II", Proc. of 7th Symp. on Acc. Science and Technology, Osaka (1989) p. 80

[12] F. M. Gardner "Phaselock Techniques", John Wiley & Sons, Chapter 2.

Figure captions

Fig. 1 Block diagram of low level RF system at TARN II.

Fig. 2 Timing chart of RF system at TARN II.

Fig. 3 Block diagram of phase lock loop (PLL).

Fig. 4-a The absolute value of $\phi_0(\omega)/\phi_r(\omega)$ are illustrated against the normalized angular frequency ω/ω_n. The parameter ζ, damping factor, is varied from 0.0 to 1.0 with 0.2 step.

Fig. 4-b Indicial response of the second order PLL. Each curve corresponds to the damping factor ζ from 0.0 to 1.0 with 0.2 step, respectively.

Fig. 5 Schematic illustration of real RF field, ideal RF field and center of bunch. u_0 denotes the phase difference between the real and the ideal RF, u_b between the bunch center and the ideal RF and v between the bunch center and real RF.

Fig. 6 The ratio of the amplitude of phase oscillations $\Delta\phi_v(= u_b-\phi_s)$ to u_0, is plotted against the angular frequency.

Fig. 7 Internal model of RF acceleration. The equations of synchrotron scillations are Laplace transformed with parameter s.

Fig. 8 Total feedback loops including the internal model. Radial position feedback loop, phase feedback loop and the programmed functional voltage, are applied to VCO.

Fig. 9 The shift of closed orbit due to the error of RF frequency, dR/df_{RF} are plotted against the acceleration time. The parameters are 1) open loop, 2) $\zeta = 0.6$, $K_r = 0.005$ and 3) $\zeta = 0.6$, $K_r = 0.05$, respectively. Beam kinetic energy T and synchrotron oscillation frequency f_s are also given.

Fig. 10 Calculated values of various RF parameters for proton beams. Notations are same as in Fig. 9.

Fig. 11 Indicial response of the phase loop without radial loop. Damping factor ζ are varied from - 1.0 to 5.0.

Fig. 12 Frequency responses of closed orbit shift at the injection energy and top energy, are plotted for two cases, one for the radial loop is absent $K_r = 0.0$ and the other $K_r = 0.005$. The damping factor ζ of the phase loop is 0.6 for both cases.

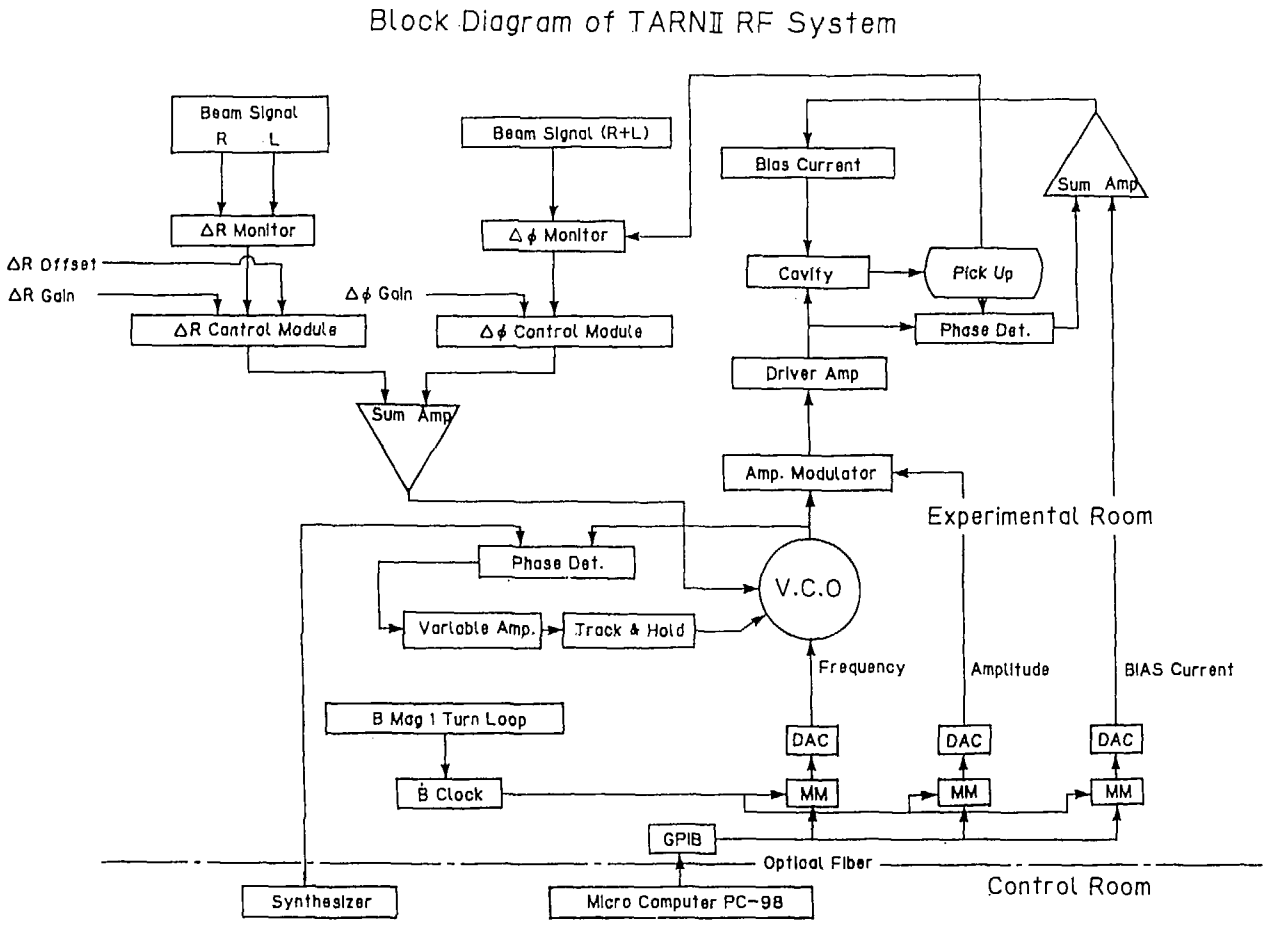
Block Diagram of TARNII RF System
Beam Signal
R L
Beam Signal (R+L)
Bias Current
Sum Amp
ΔR Monitor
Δφ Monitor
ΔR Offset
ΔR Gain
Δφ Gain
Cavity
Pick Up
ΔR Control Module
Δφ Control Module
Phase Det.
Driver Amp
Sum Amp
Amp. Modulator
Experimental Room
Phase Det.
V.C.O
Variable Amp.
Track & Hold
Frequency
Amplitude
BIAS Current
B Mag 1 Turn Loop
DAC
DAC
DAC
Ḃ Clock
MM
MM
MM
GPIB
Optical Fiber
Control Room
Synthesizer
Micro Computer PC-98

Fig. 1

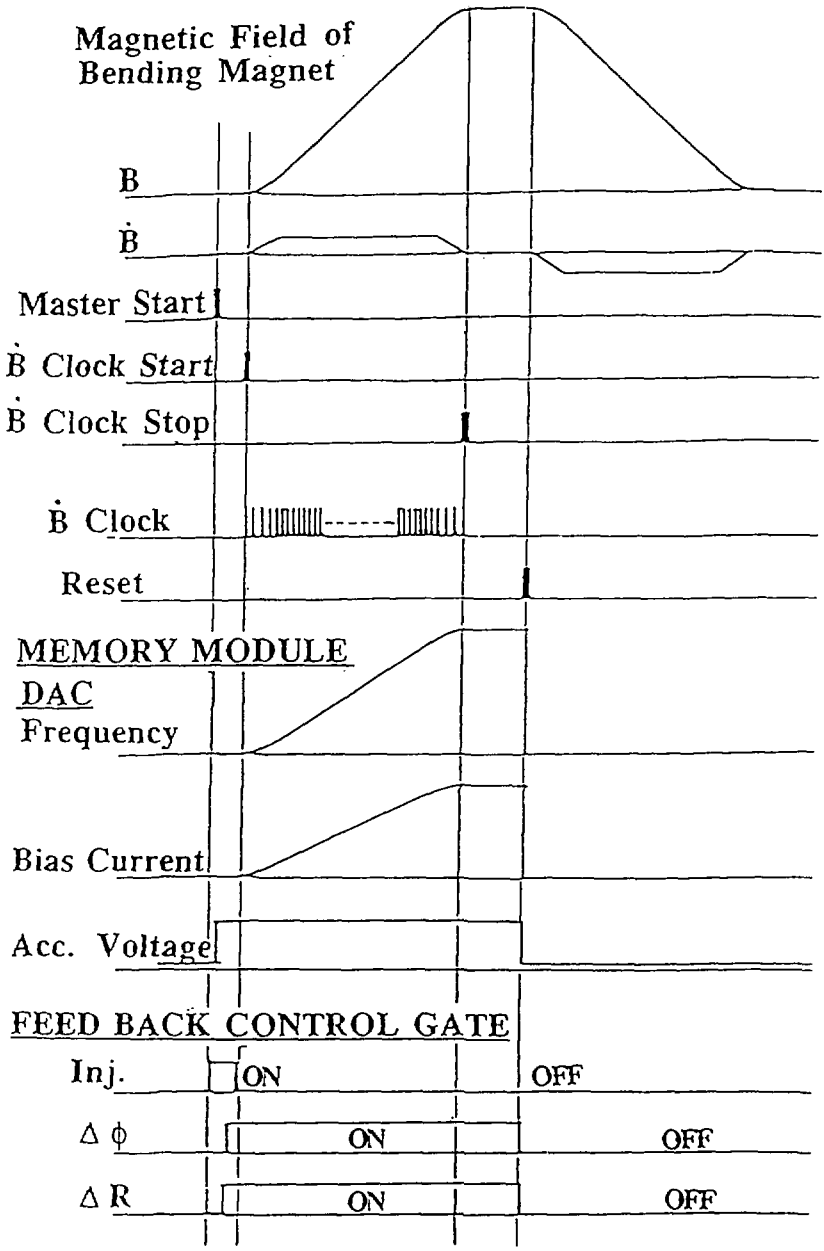
Magnetic Field of
Bending Magnet
B
Ḃ
Master Start
Ḃ Clock Start
Ḃ Clock Stop
Ḃ Clock
Reset
MEMORY MODULE
DAC
Frequency
Bias Current
Acc. Voltage
FEED BACK CONTROL GATE
Inj.
ON
OFF
Δ ϕ
ON
OFF
Δ R
ON
OFF

Fig. 2

BASIC SYSTEM OF PLL

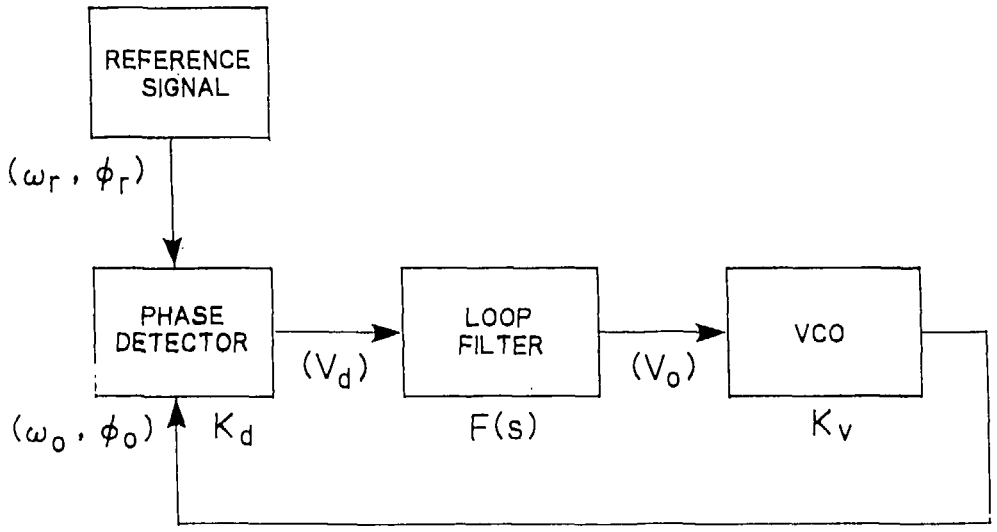

$$\frac{\phi_o(s)}{\phi_r(s)} = \frac{K_d K_v F(s)}{s + K_d \cdot K_v \cdot F(s)}$$

Fig. 3

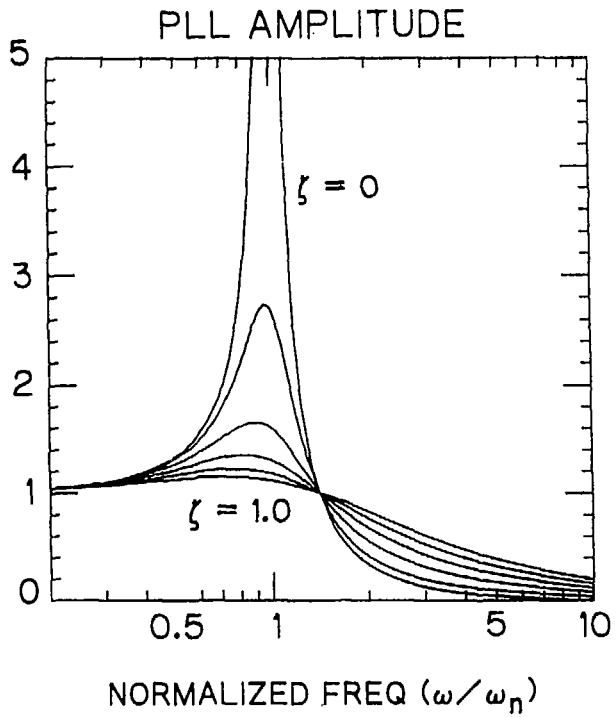
PLL AMPLITUDE
5
4
3
2
1
0
ζ = 0
ζ = 1.0
0.5
1
5
10
NORMALIZED FREQ (ω/ωn)

Fig. 4-a

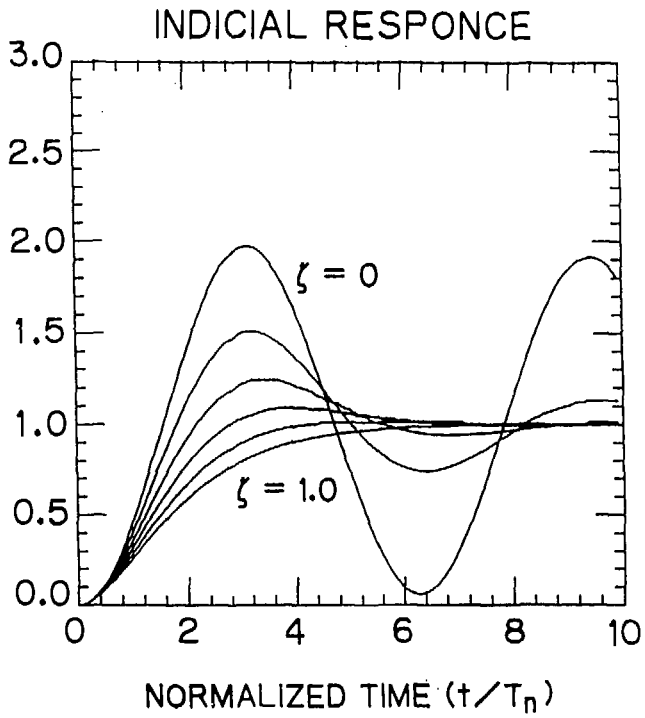
INDICIAL RESPONCE
3.0
2.5
2.0
1.5
1.0
0.5
0.0
ζ = 0
ζ = 1.0
0
2
4
6
8
10
NORMALIZED TIME (t/Tn)

Fig. 4-b

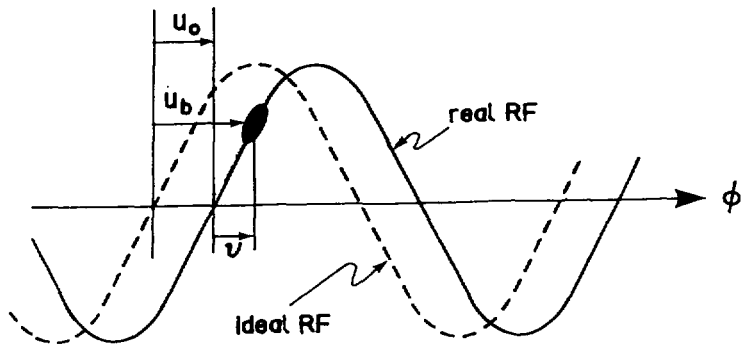
u_o
u_b
real RF
ϕ
v
ideal RF

Fig. 5

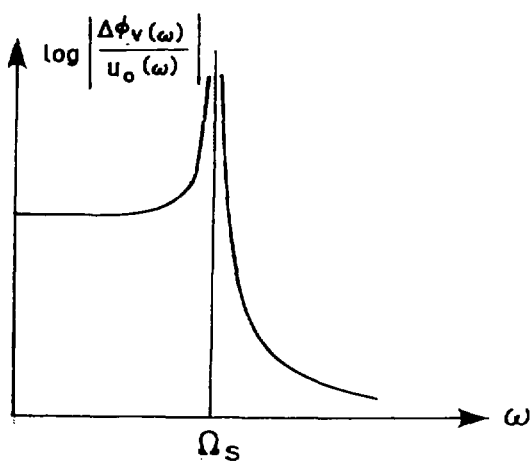
$\log \left| \frac{\Delta\phi_v(\omega)}{u_o(\omega)} \right|$
ω
Ω_s

Fig. 6

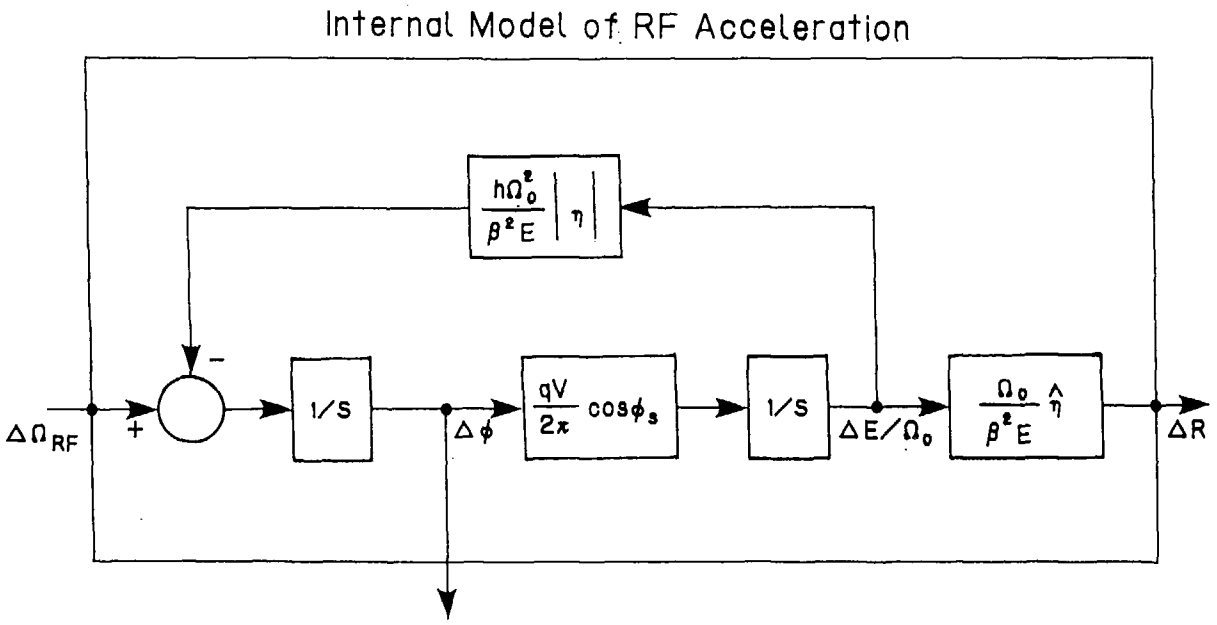
Internal Model of RF Acceleration
$\frac{h\Omega_0^2}{\beta^2 E}|\eta|$
$\Delta\Omega_{RF}$
+
−
1/S
$\Delta\phi$
$\frac{qV}{2\pi}\cos\phi_s$
1/S
$\Delta E/\Omega_0$
$\frac{\Omega_0}{\beta^2 E}\hat{\eta}$
ΔR

Fig. 7

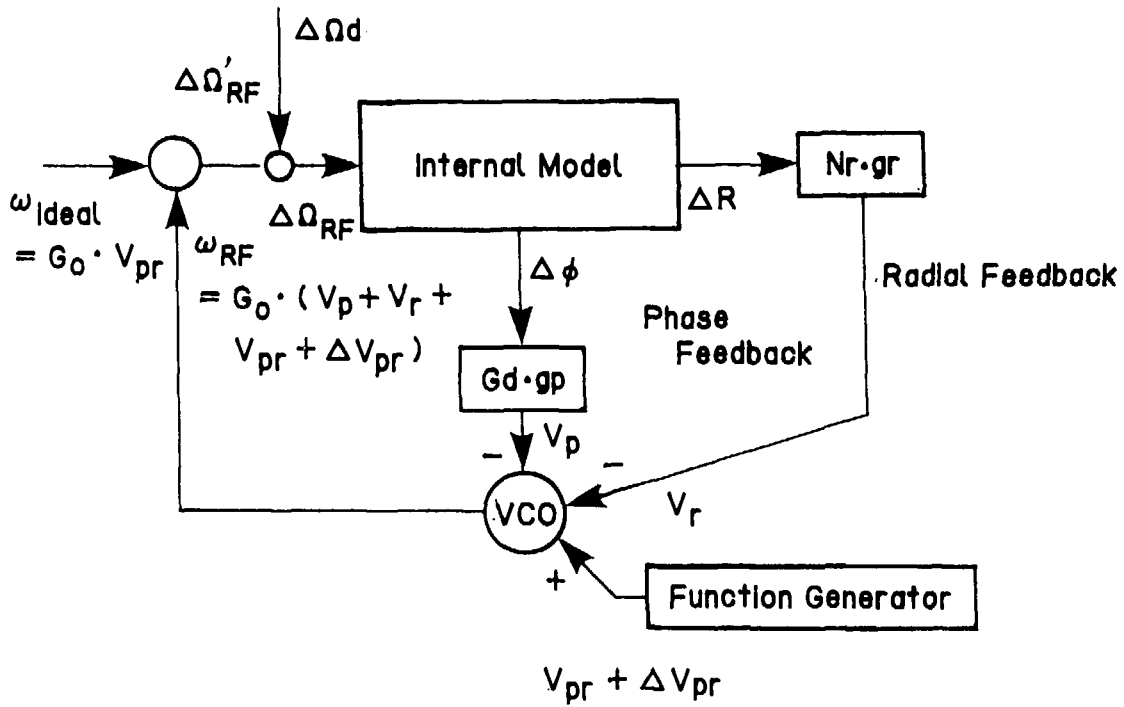
ΔΩd
ΔΩ'RF
Internal Model
Nr·gr
ΔR
ωIdeal
= Go · Vpr
ΔΩRF
ωRF
= Go · (Vp + Vr +
Vpr + ΔVpr)
Δφ
Radial Feedback
Phase
Feedback
Gd·gp
Vp
VCO
Vr
Function Generator
Vpr + ΔVpr

Fig. 8

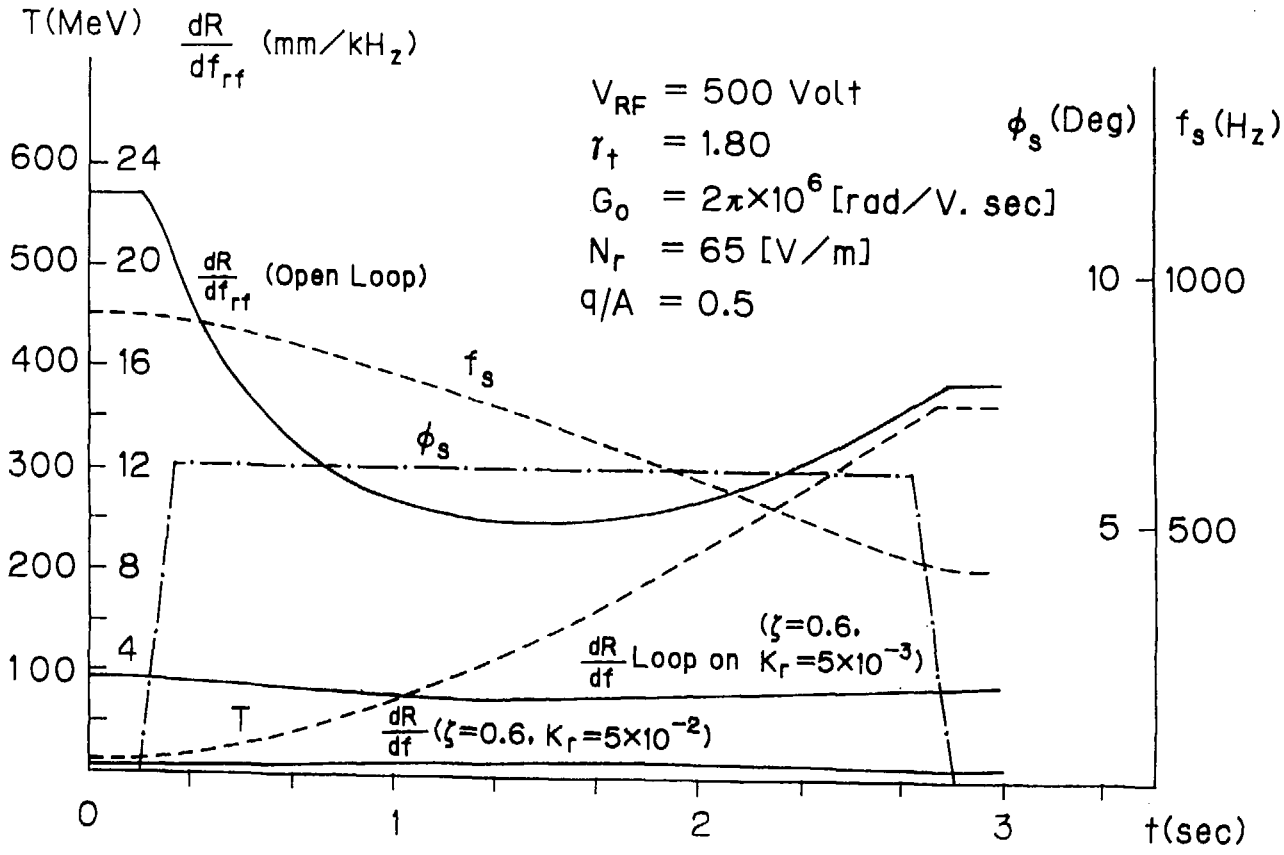
T(MeV)
dR/df_rf (mm/kH_z)
V_RF = 500 Volt
γ_t = 1.80
G_0 = 2π×10^6 [rad/V. sec]
N_r = 65 [V/m]
q/A = 0.5
φ_s (Deg)
f_s (H_z)
600
500
400
300
200
100
24
20
16
12
8
4
10
5
1000
500
dR/df_rf (Open Loop)
f_s
φ_s
(ζ=0.6, dR/df Loop on K_r=5×10^-3)
T
dR/df (ζ=0.6, K_r=5×10^-2)
0
1
2
3
t(sec)

Fig. 9

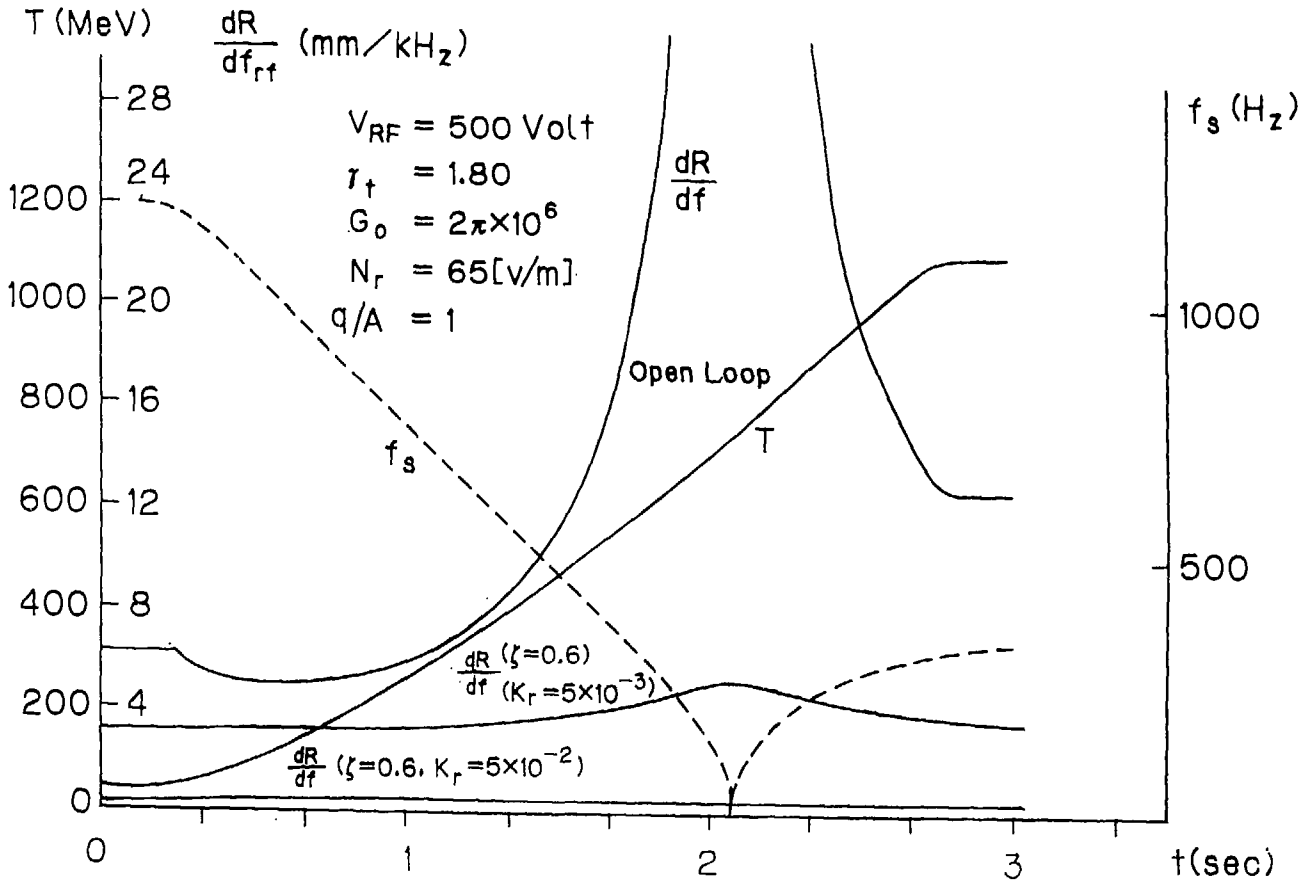
T (MeV)
dR/df_rf (mm/kHz)
f_s (Hz)
V_RF = 500 Volt
γ_t = 1.80
G_0 = 2π×10^6
N_r = 65[v/m]
q/A = 1
dR/df
Open Loop
T
f_s
dR/df (ζ=0.6)
dR/df (K_r=5×10^-3)
dR/df (ζ=0.6, K_r=5×10^-2)
1200
1000
800
600
400
200
0
28
24
20
16
12
8
4
0
1000
500
0
1
2
3
t(sec)

Fig. 10

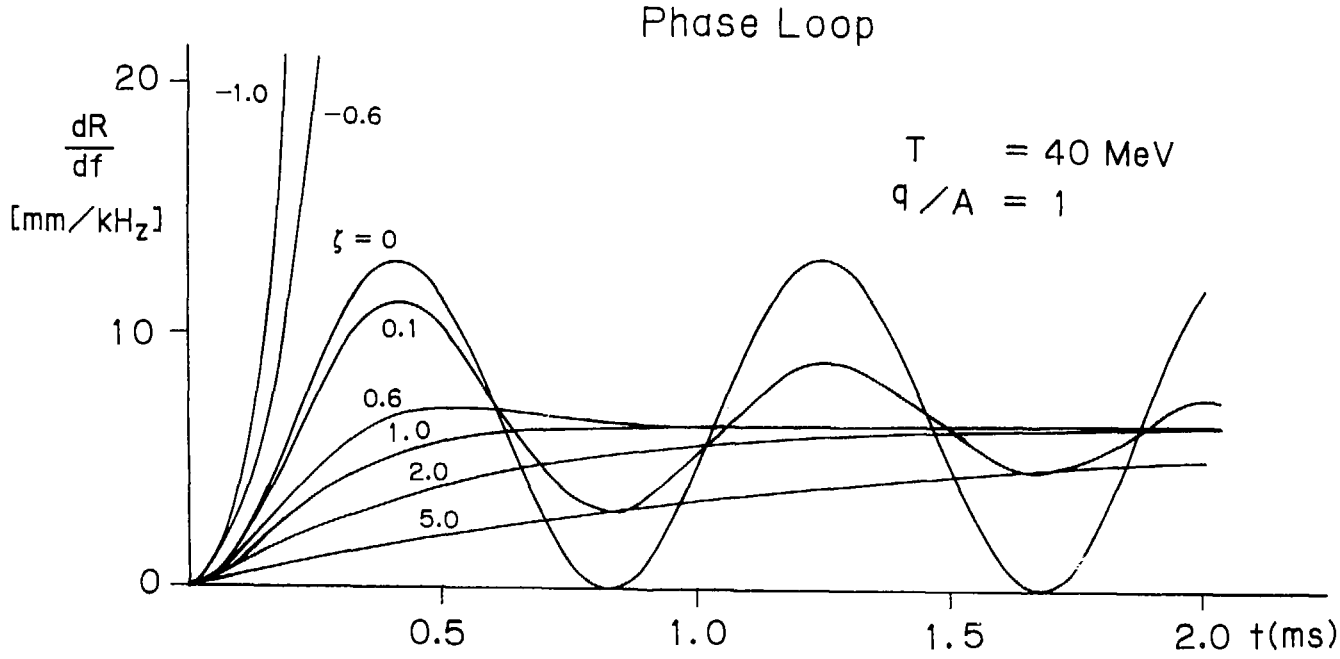
Phase Loop
20
10
0
dR/df
[mm/kHz]
-1.0
-0.6
ζ = 0
0.1
0.6
1.0
2.0
5.0
T = 40 MeV
q/A = 1
0.5
1.0
1.5
2.0 t(ms)

Fig. 11

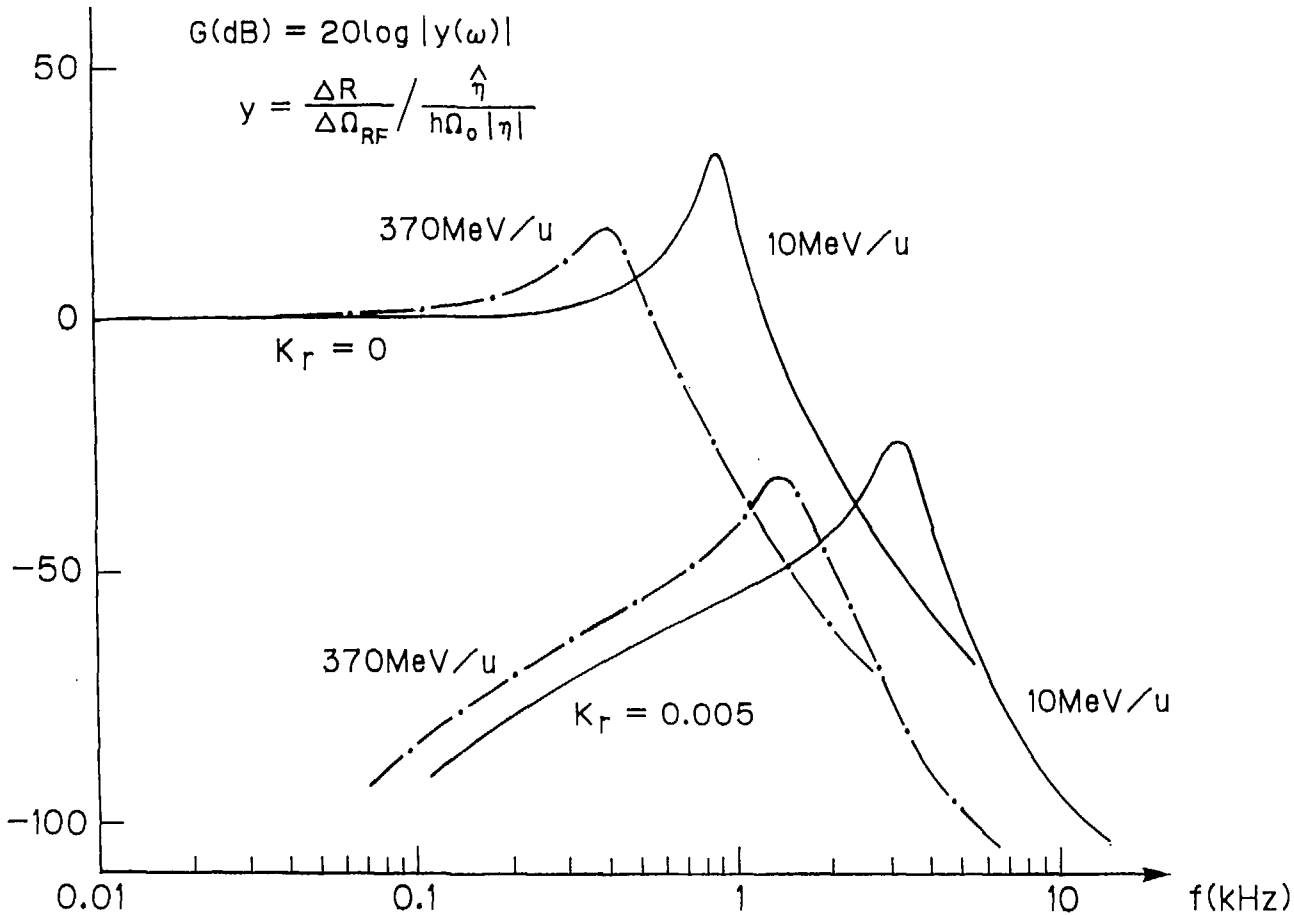
G(dB) = 20log |y(ω)|
y = ΔR/ΔΩ_RF / η̂/hΩ_o|η|
50
0
−50
−100
370MeV/u
10MeV/u
K_r = 0
370MeV/u
K_r = 0.005
10MeV/u
0.01
0.1
1
10
f(kHz)

Fig. 12